

PREPRINT

Author-formatted, not peer-reviewed document posted on 30/03/2026

DOI: <https://doi.org/10.3897/arphapreprints.e193027>

Discovery of spectabilide A, a new cytotoxic cyclic lipodepsipeptide from *Stanjemonium spectabile* revealed by OSMAC-guided metabolomics

 Gioele Pecin,  Victor Gonzalez-Menendez, Jesus Martin Serrano, Frederick Annang, Thomas Andrew Mackenzie,  Fernando Reyes,  Olga Genilloud

Title

Discovery of spectabilide A, a new cytotoxic cyclic lipodepsipeptide from *Stanjemonium spectabile* revealed by OSMAC-guided metabolomics.

Running head

Novel cyclic lipodepsipeptide from *S. spectabile*

Keywords

natural products, cyclic lipodepsipeptides, cytotoxicity, fungal epiphyte, metabolomics, mycotoxins, OSMAC, *Stanjemonium spectabile*

Authors

¹Gioele Pecin (<https://orcid.org/0009-0009-5693-0200>), ¹Victor Gonzalez-Menendez (<https://orcid.org/0000-0001-9859-6284>), ¹Jesus Martin (<https://orcid.org/0000-0001-7487-2790>), ¹Frederick Annang (<https://orcid.org/0000-0002-3014-2750>), ¹Thomas Andrew Mackenzie (<https://orcid.org/0009-0000-4297-6966>), ¹Fernando Reyes (<https://orcid.org/0000-0003-1607-5106>), ¹Olga Genilloud (<https://orcid.org/0000-0002-4202-1219>)

¹Fundación MEDINA, PTS Health Sciences Technology Park, Granada, Spain.

Author contributions

Gioele Pecin: conceptualization, methodology, investigation, formal analysis, writing – original draft, writing – review and editing. Victor Gonzalez-Menendez: methodology, investigation, writing – review and editing. Jesus Martin: methodology, investigation, formal analysis. Frederick Annang: methodology, investigation, formal analysis. Thomas Andrew Mackenzie: methodology, investigation, writing – review and editing. Fernando Reyes: conceptualization, formal analysis, supervision, writing – review and editing. Olga Genilloud: conceptualization, supervision, writing – review and editing.

Funding statement

This project has received funding from the European Union’s Horizon Europe programme under the Marie Skłodowska-Curie grant agreement No 101072485.

Conflict of interest

The authors declare no conflict of interest.

Data availability statement

The data presented in this study are available on request from the corresponding author.

Abstract

The biosynthetic potential of the fungal epiphyte *Stanjemonium spectabile*, isolated from the endemic plant *Bupleurum gibraltarium* (Granada, Spain), was investigated combining OSMAC (One Strain, Many Compounds) and metabolomic approaches. A total of 78 cultivation conditions were evaluated using different media formulations based on substrate utilization profiles obtained from Biolog FF microplates™. Chemical dereplication and MS/MS-based molecular networking revealed the production of a broad array of mycotoxins and bioactive compounds, including a novel cyclic lipodepsipeptide with a molecular formula of C₂₈H₄₈N₄O₇, spectabilide A.

Spectabilide A, composed of three amino acids and a hydroxylated aliphatic side chain, displayed potent cytotoxic activity against five human cancer cell lines, particularly against breast adenocarcinoma MCF-7 (ED₅₀ = 0.11 μM). Phylogenetic and chemotaxonomic analyses further supported the reassignment of *S. spectabile* to the *Trichothecium* clade. These findings highlight the potential of underexplored fungal taxa and cultivation strategies for the discovery of novel bioactive scaffolds and provide new insights into the chemical ecology and taxonomy of *Stanjemonium spectabile*.

Introduction

Plant-associated fungi have proved to be a relevant source for the production of bioactive molecules, including antibiotics, phytohormones and pesticides, many of them generated in response to the interactions with their host (Hashem et al., 2023). Camptothecin (Chandra, 2012), beauvericin (Al Samra et al., 2025), phaeofungin (Singh, et al., 2013), jesterone (Li et al., 2001) and phomoxanthone (Böhler et al., 2018) are just a few examples of compounds isolated from plant-associated fungi that show a strong cytotoxic or antimicrobial activity. Bioprospections of endemic and rare xerophytic plants were carried out on the arid zones of Andalusia (Spain), revealing that most of the fungi associated to the plants in this area are yet to be discovered (Bills et al., 2012; González-Menéndez et al., 2018). The presence of many endemic plants in these areas or poorly represented elsewhere suggests the possibility of discovering new plant associated fungi, as potential producers of new secondary metabolites (SMs). Despite their metabolic biosynthetic potential, it is well established that most of natural products biosynthetic pathways remain inactive in standard laboratory conditions, requiring novel methods to activate this cryptic metabolism (Scherlach and Hertweck, 2009). One of the most successful culture-based strategies to enhance a fungus chemical diversity is certainly the “one strain - many compounds (OSMAC)” approach (Bode et al., 2002). The strategy consists of systematically changing the cultivation parameters, thereby forcing the studied microorganism to adapt, eventually expressing genes that are activated only under precise environmental conditions. The OSMAC approach has proven to be effectively activating silent genes in several fungal species, including plant-associated fungi (Scherlach and Hertweck, 2009; Farinella et al., 2021; Hewage et al., 2014; Paranagama et al., 2007).

Along with the OSMAC approach, other strategies to stimulate the production of SMs in filamentous fungi have been studied in the last decade such as, the addition of adsorptive polymeric resins and epigenetic modifiers to the cultivation medium. Adding small amounts of adsorptive polymeric resins, such as XAD-16 and HP-20, to the fermentation media can, in fact, improve the production of certain metabolites by capturing them, preventing both their degradation and toxic effects for the cell and preventing any negative regulatory effect by the final product (Marshall et al. 1990; Phillips et al. 2013; González-Menéndez et al. 2014). On the other hand, it has been demonstrated that the perturbation of the normal state of chromatin in filamentous fungi can interfere with its regulatory functions, thus sometimes leading to the activation of cryptic regions of the chromosome (Brosch et al., 2008). Epigenetic modifiers like the DNA methyltransferase (DNMT) inhibitor hydralazine hydrochloride or the histone deacetylase (HDAC) inhibitor suberoylanilide hydroxamic acid (SAHA) have been successfully used to modulate the chromatic dynamics and stimulate the expression of silent genes (Scherlach and Hertweck, 2009; Cichewicz, 2010; González-Menéndez et al., 2016). Finally, the dereplication of known molecules is a key process in natural product discovery, especially important to avoid the re-discovery issue. Chemical dereplication of known molecules in the extracts is easily achieved with the current, relatively low cost and sensitive analytical techniques, using in-house databases of UV, HR-MS and MS/MS spectral data. In addition to in-house databases, the advent of open-access databases and networking tools like GNPS have allowed to analyse whole datasets against global libraries. (Greco et al., 2019; Kildgaard et al., 2014; Wang et al., 2016)

During our bioprospecting campaign to collect plant-associated fungi in the arid areas of Andalusia, a fungal strain initially identified as *Stanjemonium spectabile* was isolated as an epiphyte of *Bupleurum gibraltarium*, an endemic plant in southern Spain and Morocco. The fact that the fungus was unusually isolated as epiphyte, if compared to other soil borne *Stanjemonium* species, was what pushed us to investigate the metabolic potential of this isolate and its holotype strain CBS 340.70T following an OSMAC approach. Phylogenetic, metabolic, and chemotaxonomic data obtained in this study support a reclassification of *S. spectabile* CF-278320 and its holotype CBS 340.70T within the *Trichothecium* genus (Hou, L.W., 2023). The discovery and characterization of a novel lipodepsipeptide with biological activity against different cancer cell lines is also presented in this work.

Methods

Strain isolation and identification

The epiphyte fungal strain CF-278320 was directly isolated from conidiophores developed on dead leaves of the endemic plant *Bupleurum gibraltarium* collected in Embalse de Canales, Granada, Spain in July 2011 by incubation in a moist chamber. The isolate was cultured on YM agar (malt extract 10 g, yeast extract 2 g, agar 20 g, 1000 mL distilled H₂O) for 14 days at 22°C, to study the macroscopic and microscopic characteristics. Strain designated with unique ID (CF-278320), was preserved as frozen conidia and mycelia in 10% glycerol at -80 °C and maintained in Fundación MEDINA's fungal culture collection. DNA extraction, PCR amplification and DNA sequencing were performed as previously described (González-Menéndez et al., 2017). DNA sequence of

the complete ITS₁-5.8S-ITS₂-28S region or independent ITS and partial 28S rDNA sequences were compared with sequences at GenBank®, the NITE Biological Resource Center (<http://www.nbrc.nite.go.jp>) and CBS strain database (<http://www.westerdijkinstitute.nl>) by using the BLAST® application.

Phylogenetic analysis

To determine the phylogenetic position of our isolate, sequences from previous work on the *Acremonium* phylogenetic overview and revision of *Gliomastix*, *Sacrocladium*, and *Trichothecium* (Summerbell *et al.* 2011) and other available related sequence were downloaded from GenBank (<https://www.ncbi.nlm.nih.gov/genbank/>) to generate the phylogenetic tree. Species and genus affinities of *Stanjemonium spectabile* were inferred from a Bayesian analysis using the Markov Chain Monte Carlo (MCMC) approach with MrBayes 3.0163. To improve mixing of the chains, four incrementally heated simultaneous Monte Carlo Markov chains were run over 2×10^6 generations. Hierarchical likelihood ratio tests with the MrModeltest® 2.2 software (Nylander, 2004) were used to calculate the Akaike Information Criterion (AIC) of the nucleotide substitution models. The model selected by AIC for the alignment was GTR + I + G that is based on six classes of substitution types, a portion of invariant alignment positions and mean substitution rates, varied across the remaining positions according to a gamma distribution. The MCMC processes were followed by a Dirichlet process prior (DPP) to obtain the substitution rates and nucleotide frequencies, and a unification of the rate parameter for the gamma distribution. The MCMC analysis was performed using a sampling frequency parameter of 100 and the first 1.000 trees were discarded before the majority rule consensus tree was calculated. In addition, Maximum Likelihood method (ML) and ultrafast bootstrap support values for phylogenetic trees were assessed calculating 1000 replicates with IQ-TREE software (Nguyen *et al.*, 2014). All parameters were estimated with this software (TIM2e+G4 nucleotide substitution model was selected), assuming a shape parameter of the Invar + Gamma distributed substitution rates (gamma shape alpha = 0.4605) to accommodate rate variations among sites and an estimation of nucleotide frequencies as A = 0.25, C = 0.25, G = 0.25 and T = 0.25.

Nutritional requirements assay using Biolog FF MicroPlates

The FF MicroPlates™ (Biolog, Hayward, CA) were used to study the nutritional requirements of the strains. FF MicroPlates consists of a panel of 96 wells containing different carbon and nitrogen sources, including monosaccharides, poly- and oligosaccharides, and nitrogen-containing compounds (amino acids, amines, etc.). The redox dye Iodonitrotetrazolium violet (INT) present in the wells is used to colorimetrically measure the increase in metabolic activity due to the consumption of carbon sources. Through an irreversible reaction, the INT dye is converted to formazan, which has an absorbance maximum at 490 nm. In this way, an increase in metabolic activity in the presence of a given substrate can be measured by the increase in absorbance (Papaspyridi *et al.*, 2010). By additionally measuring the absorbance at 750 nm, length at which the mycelium spectrum of absorbance is higher, the corrected values of metabolic activity can be obtained by subtracting the measurements at 490 nm from those at 750 nm (Kubicek *et al.*, 2003).

To prepare the FF MicroPlates cultures were inoculated on 90 mm petri dishes with the nutrient-deficient media SNA (Paredes, 2024) and CMA for 14 - 21 days to stimulate sporulation. Highly sporulating cultures were harvested by scraping the surface of the plate with sterile plastic loops and the addition of Tween 80 saline solution (Tween 80 2.5 % v/v, NaCl 0.5 % w/v). Spores were filtered, centrifuged, counted in Neubauer chamber and resuspended in carboxymethyl cellulose (CMC) 0.5 % v/v to obtain a 10^6 spores/mL suspension, subsequently used to inoculate 100 μ L per well. FF MicroPlates were incubated in the dark at 25 °C and 70% RH for 96 hours, recording the absorbance values at 24, 48, 72, and 96 hours. Absorbance was measured in an ENVISION™ Multilabel Reader spectrofluorometer (PerkinElmer, Waltham, MA, USA).

Fungal fermentations

Fresh cultures of the *S. spectabile* strains were obtained by collecting pure cultures from -80 °C glycerol stocks and growing them on 55 mm petri dishes with 10 mL YM (yeast extract Difco™ 1 g, malt extract Difco™ 10 g, agar 20 g, and 1000 mL deionized H₂O) at 22°C for 14–20 days. All production media used for the OSMAC approach, and the solid-state fermentation time course were inoculated from a culture in SMYA seed medium grown for 7 days at 22 °C in an orbital shaker (200 rpm; 1.5 cm throw) and prepared as previously described (Georgousaki et al., 2020).

Eight of the media selected for the OSMAC study were already described in literature: BRFT, CYS80, DEX-SOY, M104T, MV8, Wheat-1, WS80, and YES (Table 1). The remaining seven media were designed specifically for this experiment: DEGSY, FGY-2, FOF, SM, SXSX, XYFUGA, YEC (Table 1). All OSMAC fermentations were prepared in 40 mL EPA vials with 10 mL of each medium, inoculated with 0.3 mL of seed culture and incubated at 22 °C, 70% RH, only shaking the submerged cultures at 220 rpm. The epigenetic modifier SAHA was added at a concentration of 100 μ M, and polymeric resin XAD-16 at a concentration of 3 % v/v and prepared as previously described by González-Menéndez et al. in 2014. The solid-state fermentations based on rice (BRFT) and wheat (Wheat-1) were inoculated using 1mL of SMYA inoculum and incubated in static conditions for at 22°C, 70% RH.

Table 1 Culture media composition.

Medium	Components (per litre)	Reference
BRFT	Brown rice (200g), base liquid (400mL), Bacto™ Yeast Extract (10g), sodium tartrate (5g), KH ₂ PO ₄ (5g)	Peláez et al., 2000
CYS80 (+ SAHA)	Sucrose (80g), yellow corn meal (50g), Bacto™ Yeast Extract (1g)	Suay et al., 2000
DEGSY	Dextrin from potato starch (40g), L-glutamic acid (38g), soybean flour (1g), Bacto™ Yeast Extract (5g)	
Dex-Soy (+ XAD-16)	Dextrin (40g), glucose (10g), malt extract (5g), ploypeptone (5g), soybean flour (5g), Bacto™ Yeast Extract (2g), KH ₂ PO ₄ (1g)	Georgousaki et al., 2019
FGY-2 (+ XAD-16)	Fructose (40g), monosodium glutamate (8g), Bacto™ Yeast Extract (8g), L-glutamic acid (15g), KH ₂ PO ₄ (1.5g), MgSO ₄ •7H ₂ O (0.4g), trace elements (10mL: FeSO ₄ •7H ₂ O 1g/L, MnSO ₄ •H ₂ O 1 g/L, ZnSO ₄ •7H ₂ O 0.4 g/L, CaCl ₂ •2H ₂ O 0.1 g/L, HBO ₃ 0.056 g/L, CuCl ₂ •2H ₂ O 0.025 g/L, (NH ₄) ₆ Mo ₇ O ₂₄ •4H ₂ O 0.019 g/L, HCl (12 N) 50 mL/L)	
FOF (+ SAHA)	Fructose (75g), oat flour (15g), Bacto™ Yeast Extract (5g), L-glutamic acid (4g), MES (16.2g), adjusted to pH 6.0	
M104T	Sorbitol (100g), glucose (40g), glutamic acid (10g), KH ₂ PO ₄ (0.5g), MgSO ₄ (0.5g), Bacto™ Yeast Extract (3g), DL-tryptophan (0.8g)	Bacon, 1988
MV8 (+ SAHA)	Maltose (75g), V-8 juice (200mL), soy flour (1g), L-proline (3g), MES (16.2g)	González-Menéndez et al., 2014
SM (+ XAD-16)	D-sorbitol (100g), glucose (40g), succinic acid (10g), KH ₂ PO ₄ (1g), MgSO ₄ •7H ₂ O (0.3g), Bacto™ Yeast Extract (1g), trace elements (5mL: citric acid 0.5 g/L, Fe(NH ₄) ₂ (SO ₄) ₂ •5H ₂ O 0.1 g/L, ZnSO ₄ •7H ₂ O 0.5 g/L, MnSO ₄ •H ₂ O 0.005 g/L, Na ₂ MoO ₄ •2H ₂ O 0.005 g/L, CuSO ₄ •5H ₂ O 0.025 g/L), adjusted to pH 5.6	
SXSY (+ SAHA)	Soluble potato starch (40g), xylose (40g), L-serine (25g), Bacto™ Yeast Extract (5g)	
Wheat-1	Wheat grain (500g), liquid base (220mL), glycerol (2g), Bacto™ Yeast Extract (2g), sodium tartrate (10g), KH ₂ PO ₄ (1g), MgSO ₄ •7H ₂ O (1g), FeSO ₄ •7H ₂ O (0.05g)	Bills et al., 2008
WS80 (+ SAHA)	Wheat flour (50g), xylose (40g), fructose (40g)	Ondeyka et al., 2007
XYFUGA (+ XAD-16)	Xylose (40g), fructose (40g), N-acetylglucosamine (5g), L-aspartic acid (2g)	
YEC (+ XAD-16)	Bacto™ Yeast Extract (20g), D-cellobiose (150g), MgSO ₄ •7H ₂ O (0.5g), YES trace elements (1mL)	
YES (+ XAD-16)	Bacto™ Yeast Extract (20g), MgSO ₄ •7H ₂ O (0.5g), sucrose (150g) trace elements (1mL)	González-Menéndez et al., 2014

The fermentation conditions for the purification of the novel compound were performed using the best producing solid-state fermentation medium BRFT. Cultures from SMYA

seed medium were inoculated in Erlenmeyer flasks containing BRFT, testing two different formats: 50 mL medium in 250 mL flasks inoculated with 2 mL seed culture, and 100 mL medium in 500 mL flasks inoculated with 4.5 mL seed culture. The cultures were incubated under static conditions for 7, 10, 14, 17, 21, 25 or 28 days, at 22 °C and 70% RH.

Extracts harvesting and processing

EPA vial format fermentations were harvested and extracted by adding 10 mL of acetone to the 10 mL whole broth, breaking the mycelium of solid-state fermentation media like BRFT and Wheat-1 with a spatula, and shaking at 200 rpm for 3 h. The vials were centrifuged, and 12 mL of supernatant decanted into clean tubes and mixed with 0.64 mL of DMSO. Samples were then evaporated under a nitrogen stream to a volume of 3.2 mL (20% DMSO v/v) and final concentration of 2×WBE (Whole Broth Equivalent). Vials with added XAD-16 resin were extracted and evaporated a second time with 100% acetone, finally concentrating the extracted volume in the same tubes of the first extraction. Solid-state BRFT fermentations used to evaluate the best production conditions were processed by adding 1:1 v/v of acetone to the flasks, breaking the mycelia with a spatula and shaking at 200 rpm for 3 h. The fermentations were then centrifuged, and an aliquot of 20 mL was decanted into clean EPA vials to be processed as previously described.

Chemical dereplication

Extracts were analyzed by LC/MS and searched against Fundación MEDINA's proprietary database using both, LC-LRMS data searching for retention time, UV spectrum, MS(+) and MS(-), or LC-HRMS data using retention time, accurate mass, and fragmentation patterns, to dereplicate known compounds (González-Menéndez et al., 2016; Martín et al., 2014; Pérez-Victoria et al., 2016). Secondary metabolites whose predicted molecular formulae were not identified within the internal database were searched against the Dictionary of Natural Products (DNP, v25.1) and The Natural Products Atlas (Poynton et al., 2024) databases.

Metabolic analysis (MS/MS data, MN)

LC-MS/MS data were converted to mzXML format using MSConvert software (Chambers et al., 2012). With the converted data, a molecular network (MN) was created on the GNPS website (<http://gnps.ucsd.edu>). The data was filtered by removing all MS/MS fragment ions within +/- 17 Da of the precursor m/z. MS/MS spectra were window filtered by choosing only the top 6 fragment ions in the +/- 50 Da window throughout the spectrum. The precursor ion mass tolerance was set to 0.1 Da and a MS/MS fragment ion tolerance of 0.02 Da. A network was then created where edges were filtered to have a cosine score above 0.7 and more than 6 matched peaks. Further, edges between two nodes were kept in the network if and only if each of the nodes appeared in each other's respective top 10 most similar nodes. Finally, the maximum size of a molecular family was set to 100, and the lowest scoring edges were removed from molecular families until the molecular family size was below this threshold. The spectra in the network were then searched against GNPS' spectral libraries. The library spectra

were filtered in the same manner as the input data. All matches kept between network spectra and library spectra were required to have a score above 0.7 and at least 6 matched peaks (Wang et al., 2016). The results of the MN can be found at <https://gnps.ucsd.edu/ProteoSAFe/status.jsp?task=ede7a1d3c8244b0abc741acf8630c23c>. To visualize the cluster maps of the results, the data were then exported to Cytoscape® (version 3.10.3) (Shannon et al., 2003).

Purification of spectabilide A

A 1.5 L culture of *S. spectabile* in BRFT medium was extracted by addition of an equal volume of 1.5 L of Milli-Q water. The mixture was stirred to create a homogeneous aqueous suspension. This was then extracted by shaking with 1.5 L acetone in a Kuhner shaker at 200 rpm, 24°C, for 2 h. The extract was filtered, and the acetone evaporated under a heated nitrogen stream to obtain a concentrated crude. This crude was extracted two times with 1.5 L of ethyl acetate and the organic phases were combined and dried. This extract was re-dissolved in methanol and mixed with double amount of C-18 reversed-phase silica gel. The mixture was evaporated to dryness in a rotary evaporator, after which the residue was loaded onto a C-18 reversed-phase column that was eluted at 18 mL/min flow rate with a linear gradient of 5-100% CH₃CN/H₂O (total run time was 54 min). 55 fractions (20 mL each) were collected and subjected to LC/MS analysis, which confirmed the presence of spectabilide A in fraction 17. This fraction was subsequently subjected to repeated semi-preparative reversed-phase HPLC (linear gradient 5-100% CH₃CN/H₂O in 45 min, using an Agilent Zorbax SB-C18 column (9.4 × 250 mm, 5 μm) at 3.6 mL/min flow rate with UV detection at 210 and 280 nm). 3.5 mg of spectabilide A were obtained, eluting at a retention time of 22 min.

Spectabilide A. White, amorphous solid; (+)-ESI-TOF MS m/z 553.3606 [M + H]⁺ (calcd. for C₂₈H₄₉N₄O₇⁺, 553.3596); ¹H and ¹³C NMR data, see Table 2.

Marfey's analysis of the novel compound

A sample of 200 μg of pure compound was dissolved in 0.4 mL of 6 N HCl and heated at 110 °C for 16 h. The hydrolysate was then evaporated to dryness under a N₂ stream, and the residue dissolved in 100 μL of water. 100 μL of a 1% (w/v) solution of D-FDVA (N-(2,4-dinitro-5-fluorophenyl)-D-valinamide) in acetone was added to the aqueous solution of the compound hydrolysate and to a 50 μL aliquot of a 50 mM solution of each amino adipic acid enantiomer (DL mixture or L) and, after the addition of 20 μL of 1 M NaHCO₃ solution, each mixture was incubated at 40 °C, 800 rpm for 60 min. After the incubation, the reactions were quenched by the addition of 10 μL of 1 N HCl, and the crude mixtures were diluted with 700 μL of acetonitrile to be analysed by LC/MS on an Agilent 1100 single quadrupole. Separations were carried out on a Waters XBridge C18 column (4.6 × 150 mm, 5 μm) maintained at 40 °C. A mixture of two solvents, A (10% acetonitrile, 90% water) and B (90% acetonitrile, 10% water), both containing 1.3 mM trifluoroacetic acid and 1.3 mM ammonium formate, was used as mobile phase under a linear gradient elution mode (25–55% B in 30 min, 55–100% B in 1 min, isocratic 100% B for 4 min) at a flow rate of 1 mL/min.

Bioactivity characterization

Bioactivity of the purified compound was evaluated against five different human cancer cell lines: human hepatocellular carcinoma HepG2 (ATCC HB-8065), breast adenocarcinoma MCF-7 (ATCC HTB-22), pancreas carcinoma MIA PaCa-2 (ATCC CRL-1420), skin melanoma A2058 (ATCC CLR-11147), and lung carcinoma A549 (ATCC CCL-185). The activity was evaluated by MTT reduction colorimetric assays (Mosmann, 1983) in a high-throughput 96-well-plate format, testing the isolated compound in triplicate, in 10-point dose-response curves with a starting concentration of 50 μ M and following $\frac{1}{2}$ serial dilutions for 72 hours, as previously described by de Pedro et al. (2012) ED₅₀ values were determined for each cell line using Genedata Screener® (Cautain et al., 2015).

General Experimental Procedures

Optical rotations were measured in a Jasco P-2000 polarimeter (JASCO Corporation, Tokyo, Japan) in methanol. 1D- and 2D-NMR spectra were recorded on a Bruker Avance III spectrometer (500 and 125 MHz for ¹H and ¹³C NMR, respectively) equipped with a 1.7 mm TCI MicroCryoProbe (Bruker Biospin, Fällanden, Switzerland). Chemical shifts were reported in ppm using the signals of the residual solvents as internal reference (δ_{H} 3.31 and δ_{C} 49.1 for CD₃OD).

LC–UV–MS measurements were carried out using an Agilent 1100 LC–MS instrument equipped with a single quadrupole detector. Chromatographic separation was achieved on a Zorbax SB-C8 column (2.1 x 30 mm, 5 μ m particle size) operated at 40 °C with a mobile-phase flow rate of 300 μ L/min. The mobile phase consisted of solvent A (water/acetonitrile, 90:10, v/v) and solvent B (water/acetonitrile, 10:90, v/v), both containing 1.3 mM trifluoroacetic acid (TFA) and ammonium formate. A linear gradient was applied from 10% to 100% solvent B over 6 min, followed by a 2 min hold at 100% B, and re-equilibration to initial conditions over 2 min. UV detection was performed using diode-array scanning across 100–900 nm with 4 nm resolution and a scan interval of 0.25 s. Ionization of the eluent was achieved via electrospray using the standard Agilent source, operated with a drying gas flow of 11 L/min at 325 °C, a nebulizer pressure of 40 psig, and a capillary voltage of 3.5 kV. Mass spectra were acquired in full-scan mode over an m/z range of 150–1500, with a scan cycle time of 0.77 s, in both positive and negative ionization modes. High-resolution ESI and tandem MS analyses were conducted on a Bruker maXis QTOF mass spectrometer interfaced with the same HPLC system, operating in positive ESI mode at a capillary voltage of 4 kV, drying gas temperature of 200 °C with a flow rate of 11 L/min, and a nebulizer pressure of 2.8 bar. External mass calibration was performed prior to analysis using TFA–Na cluster ions, with pre-run calibration achieved by direct infusion of the same standard. Analytical-grade acetone was employed for extraction procedures, while all solvents used during compound isolation were of HPLC quality.

Results

Strain isolation and identification

The strain CF-278320 was isolated as epiphyte from conidiophores developed on dead leaves of the endemic plant *B. gibraltarium* collected from arid zones of Andalucía (Embalse de Canales, Granada, Spain) during a sample collection campaign. The strain was initially cultivated on YME plates at 22 °C, showing floccose-lanose mycelium with white to pale pink colour. Formation of conidia was mainly observed on nutrient-poor media such as cornmeal agar (CMA) and synthetic nutrient agar (SNA) after approximately 14 days of cultivation. Its macroscopical characteristics, in terms of colony and conidia formation, were comparable to those previously described for *S. spectabile*, (W. Gams 1973; W. Gams et al. 1998) (Figure 1). The identification was further confirmed with the analysis of its ITS₁-5.8S-ITS₂ and 28S sequences (GenBank® accession number: PX069749.1), which revealed a 100 % similarity with *S. spectabile* CBS 340.70T.

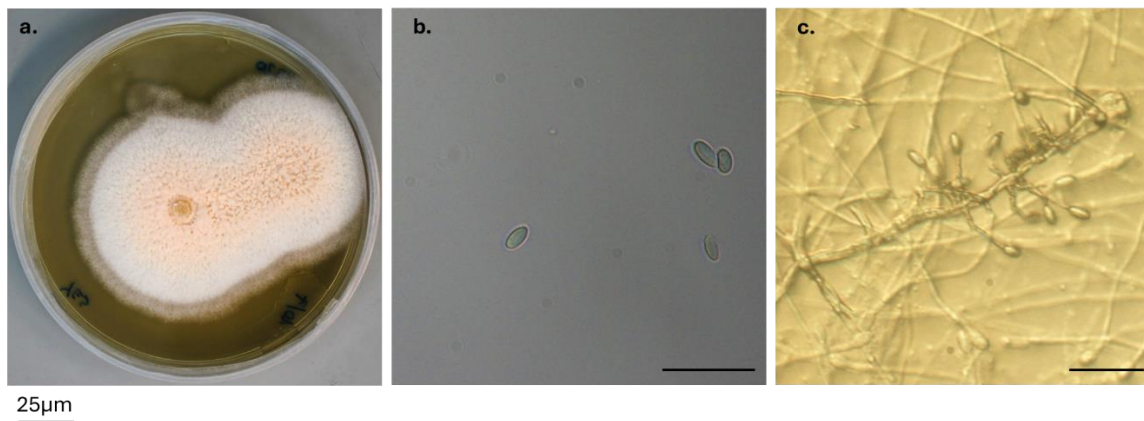


Figure 1 *A* CF-278320 colony on YME agar after 14 days of cultivation; *B* conidia from CMA observed at 14 days of cultivation; *C* *S. spectabile* CF-278320 conidiophores observed on YME medium at 21 days of cultivation.

The isolation of the strain from a plant source was however in contrast with the origin described for all other *Stanjemonium* strains from CBS collection (<https://wi.knaw.nl>), which were obtained from soil sources, except for *Stanjemonium dichromosporum*, isolated from rhizosphere, and *S. spectabile* CBS 340.70T, isolated from air samples. As previously reported by Hou et al. (2023), CBS 340.70T forms a fully supported clade with species of *Trichothecium* and clearly separates from the *Stanjemonium* clade. We therefore decided to conduct a phylogenetic analysis of CF-278320 and the holotype CBS 340.70T (Westerdijk Institute collection), including in the tree several species belonging to *Trichothecium*, *Stanjemonium*, and nearby clades, defined on ITS sequences available on NCBI. The analyses carried out with Maximum Likelihood and Bayesian models resulted in the same tree topology. In accordance with the study of Hou et al. (2023), the consensus phylogenetic tree revealed that the two strains of *S. spectabile*, along with the putative conspecific *Aphanocladium spectabile* NBRC 101148, cluster within the *Trichothecium* clade, while the other *Stanjemonium* spp. remain separated and close to the *Emerecillopsis* clade (Figure 2).

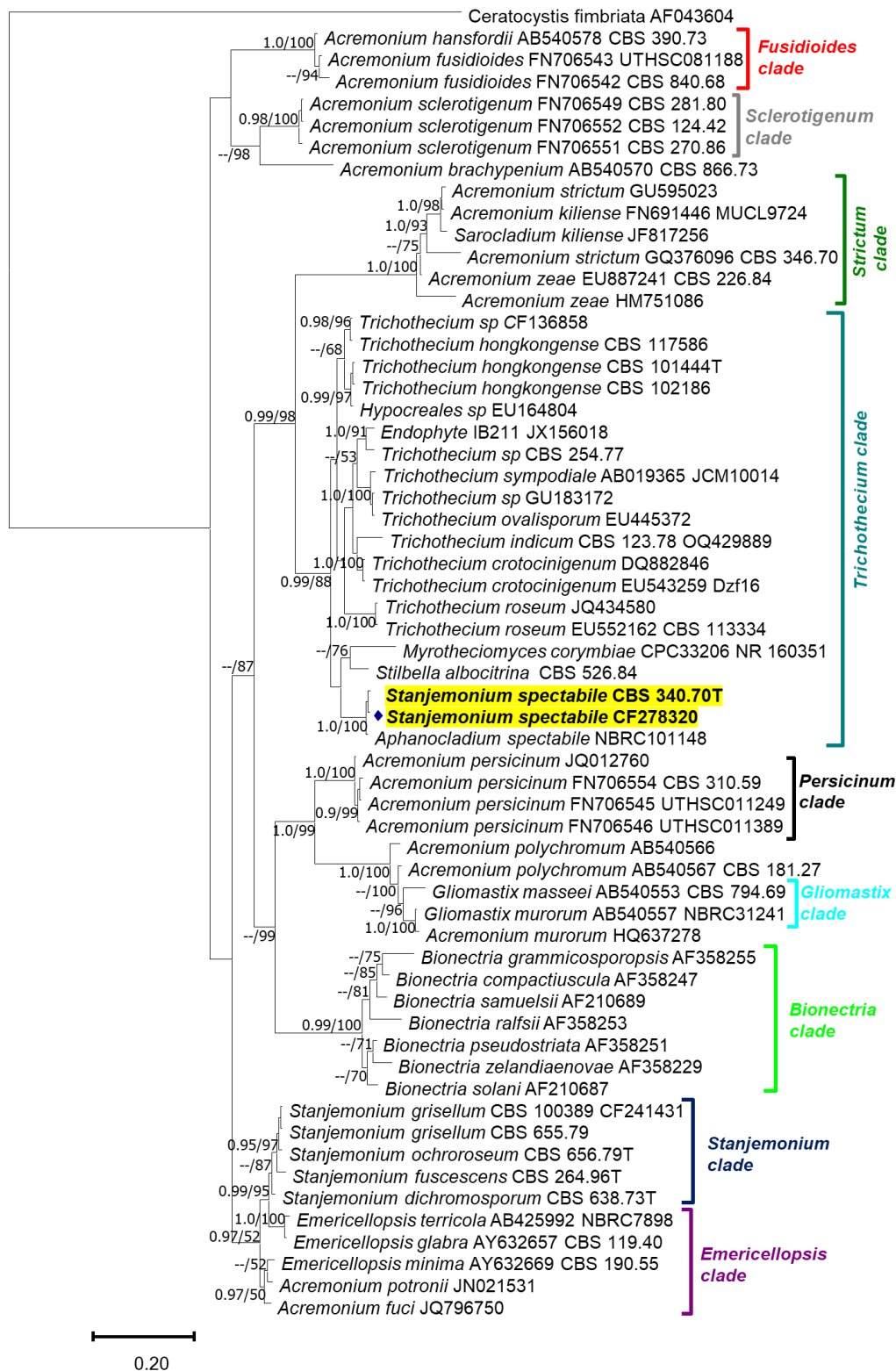


Figure 2 ITS Consensus tree based on Maximum Likelihood (ML) and Bayesian analyses. Clade probability values/ML bootstrap values are indicated respectively on the branches. Values < 0.90 are designated by "--".

Expanding *Stanjemonium spectabile* chemical diversity by OSMAC approach

The lack of genomic and metabolomic information reported in literature regarding *S. spectabile* and the results suggesting its inclusion in a different phylogenetic group far from the clade of other *Stanjemonium* strains, determined the detailed study of the biosynthetic potential of the two strains CF-278320 and CBS 340.70T following an OSMAC approach. The design and selection of the best culture media required to first investigate the nutritional requirements of the strains using FF MicroPlates. The array of substrates contained in the 96 well plates is utilized differently by each fungal species and defines the utilization preferences of each carbon and nitrogen source. The substrate utilization profiles of both strains CF-278320 and CBS 340.70T are reported in Figure S.1-4 (Supplementary material). Notably, the profiles of the two strains differ one to the other, in terms of both preferred substrates and metabolic activity (measured with a colorimetric assay). We selected carbon sources and nitrogen-containing substrates based on two criteria: the inclusion of substrates that are rapidly utilized and utilized secondarily in later stages of growth by the fungus, and the immediate commercial availability of the substrates. The ten selected carbon sources included sucrose, fructose, xylose, maltose, dextrin, glucose, D-sorbitol, D-cellobiose, N-acetyl-d-glucosamine, and glycerol. Five nitrogen-including substrates included L-proline, succinic acid, L-glutamic acid, L-aspartic acid, and L-serine. We selected eight media from literature that included some of the previously chosen carbon sources and nitrogen-containing substrates (BRFT, CYS80, DEX-SOY, M104T, MV8, Wheat-1, WS80, and YES). In addition, seven new media were specifically designed for the experiment: DEGSY, FGY-2, FOF, SM, SXSX, XYFUGA, YEC. Some of the media included complex substrates like oat (FOF), soy (DEGSY, Dex-Soy, MV8), wheat (Wheat-1, WS80), corn flour (CYS80), brown rice (BRFT), and V8 juice (MV8), while other media's main carbon sources were simple saccharides (FGY-2, M104T, SM, XYFUGA). Five media (CYS-80, FOF, MV8, SXSX, WS80) were tested in duplicate, adding in one condition the epigenetic modifier SAHA. Similarly, another six media (DEX-SOY, FGY-2, SM, XYFUGA, YEC and YES) were tested in duplicate with the addition of the adsorptive polymeric resin XAD-16 to one of the conditions (Table 1). Finally, for each of the 26 formulations mentioned above, three incubation times, 7, 14, and 21 days, were included to expand the timeframe of different metabolites production. The OSMAC-based media study globally encompassed a total of 78 fermentation conditions for each strain (CF-278320 and CBS 340.70T) (Figure S.5).

Chemical analysis of the metabolic diversity

The chemical profiles of the extracts coming from each fermentation condition were analysed by low resolution UV-LC-LRMS and, at this stage, no molecules matching our internal database were found. The UV-LC-LRMS profiles were then used to select a total of 20 conditions to be analysed with LC-HRMS and MS/MS fragmentation (Table S.1). The selection was based on the abundance and intensity of the peaks present on the single chromatograms, which indicate a higher chemical diversity in the extracts, and including at least one condition for each medium. Since the culture media containing polymeric resin XAD-16 did not present significant changes in the LC-LRMS spectra when compared with the respective control media, these conditions were not considered for further analyses.

LC-HRMS and MS/MS fragmentation analyses allowed to assign accurate molecular formulas (MFs) to the components that did not match our internal database. The

annotation of unmatched compounds was performed by searching their predicted MFs against the Dictionary of Natural Products (DNP) and The Natural Products Atlas (Poynton et al., 2024) databases. MS/MS data were also used to generate a featured-based molecular network (FBMN) using GNPS, to better visualize and interpret the dataset, as reported in Figure 3. Each node of the MN represents the m/z of a parent ion, while the edges are labelled as the differences in m/z values between the nodes. The MN revealed the presence of several clusters, including those of annotated toxins, and that of one unknown component with two possible analogues.

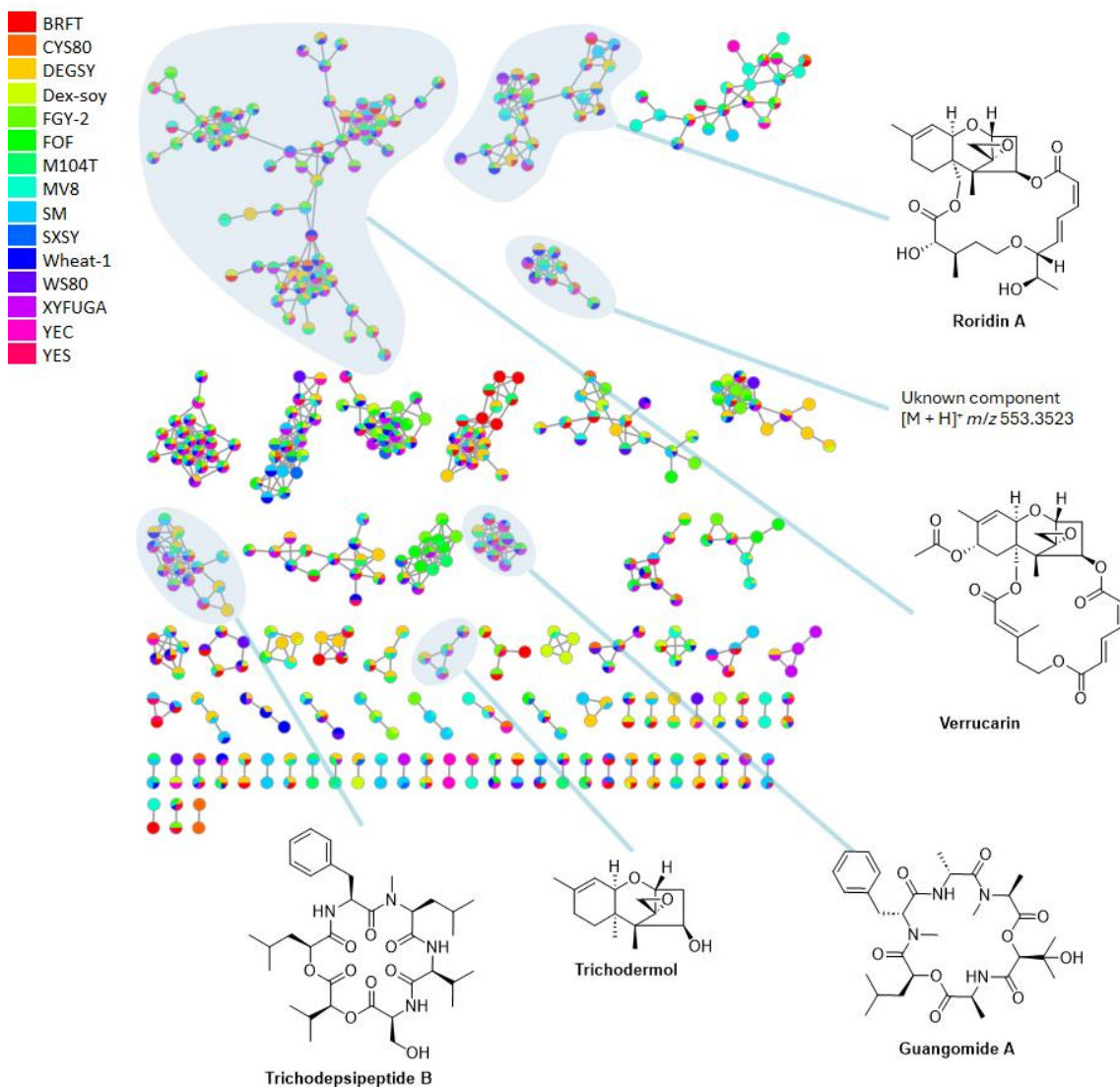


Figure 3 FBMN generated from the MS/MS data of the selected OSMAC extracts. The different media in which a single fragment is produced are represented as color-coded charts for each node. On the sides, identified clusters of the putative mycotoxins and components annotated.

Among the selected conditions, 29 components that corresponded to relevant peaks in the UV traces were annotated, and for 25 of them a putative name was given based on the predicted MFs and the database dereplication (Table S.1). Most of the putative components identified are mycotoxins, such as trichodermol (C₁₅H₂₂O₃), trichoverrol A (C₂₃H₃₂O₇), verrol (C₂₁H₃₀O₆), myrothecine C (C₂₉H₃₆O₁₁), roridin A (C₂₉H₄₀O₉),

verrucarin J ($C_{27}H_{32}O_8$), myrotoxin ($C_{29}H_{34}O_{11}$) and verrucarins L-acetate ($C_{29}H_{34}O_{10}$), being the latter present in all the extracts. Other compounds detected, including 8- α -acetoxyverrol ($C_{23}H_{32}O_8$), antibiotic TAN 1746 ($C_{28}H_{40}N_4O_6$), emerixanthone E ($C_{27}H_{30}O_9$), and cerebroside B ($C_{41}H_{77}NO_9$) are reported in literature to have antifungal or antibacterial activity (Yuan et al., 2020; Masouka et al., 2000; Fredimoses et al., 2018; Meng et al., 2011). The analysis of chemical profiles also unveiled the presence of four unknown components, three of which were only present in traces in four media. However, the fourth unknown component, with a predicted molecular formula $C_{28}H_{48}N_4O_7$ (Figure 4), showed relevant chromatographic UV_{210nm} and MS peaks in 7 of the 20 fermentation conditions. Moreover, the FBMN analysis revealed the presence of two putative analogs of the metabolite, with tentative molecular formulae of $C_{28}H_{46}N_4O_6$ and $C_{28}H_{47}N_3O_8$, produced in traces. These could correspond to a loss of H_2O in the first case, and the substitution of an $-NH_2$ group with an $-OH$ group in the second (Figure 4).

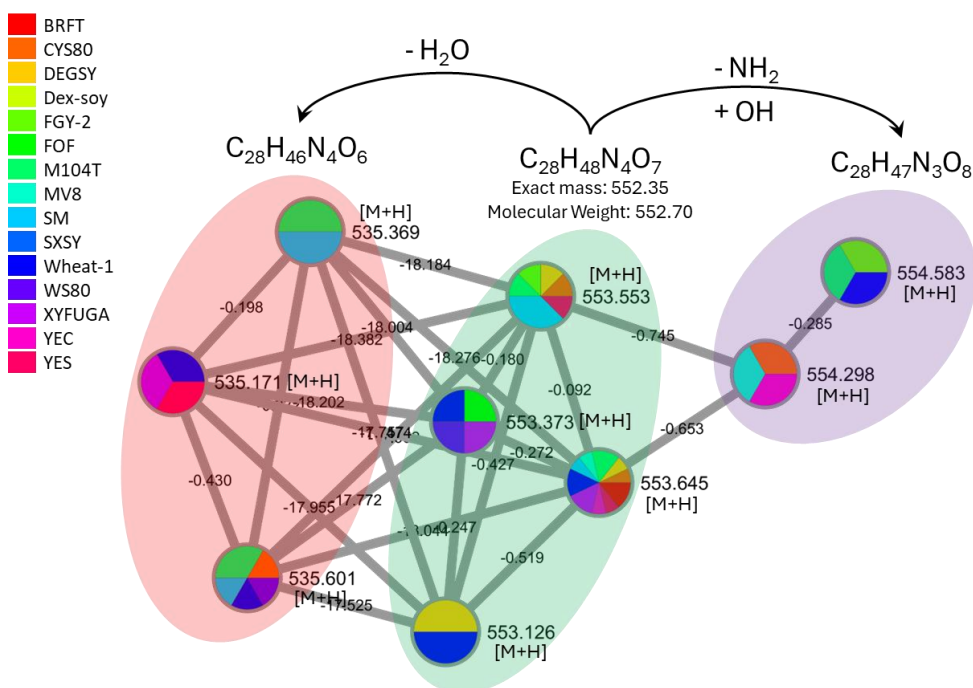


Figure 4 Cluster of the annotated unknown compound with molecular formula $C_{28}H_{48}N_4O_7$ and accurate mass of 552.35.

Changes in the production of the unknown component $C_{28}H_{48}N_4O_7$ in all conditions were determined by comparing the areas under the extracted MS chromatograms for peak EIC 553.360 ± 0.005 to their corresponding control media. The production titers of the component for strain CF-278320 were highest in the solid-state medium BRFT, followed by FOF, MV8 and YEC media (Figure 5). Production titers in the CBS 340.70T holotype strain were instead generally lower, compared to strain CF-278320. The addition of SAHA in some media slightly increased the production of the component, such as in MV8 and WS80, while the addition of XAD-16 resin increased its production in FGY-2, SM, XYFUGA and YES media, but strongly decreased it in YEC medium (Table S.1). In view of the significant amounts of this component produced in several culture media, we

focused our efforts on scaling-up the cultures and performing its isolation and structural characterization.

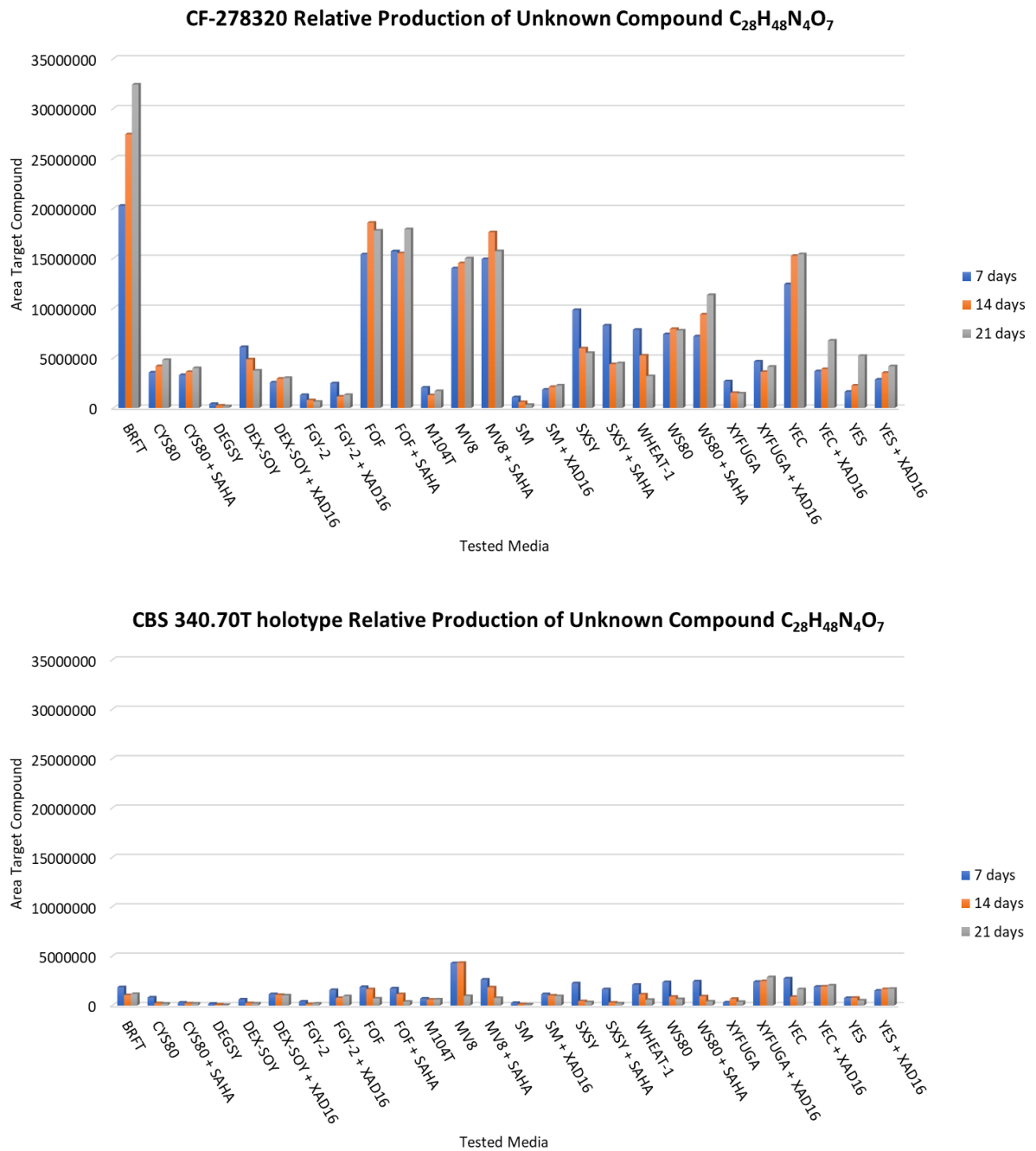


Figure 5 Relative production of the component $C_{28}H_{48}N_4O_7$ for the two strains of *S. spectabile* on the different media, represented as area under the peak of the target component ($EIC\ 553.360 \pm 0.005$)

Definition of the best cultivation conditions for the production of component $C_{28}H_{48}N_4O_7$

As mentioned above, the highest production titers of the unknown component with the molecular formula of $C_{28}H_{48}N_4O_7$ were obtained on the solid-state fermentation medium

BRFT. This medium was selected to study the production of the component over time with a time-course experiment with both strains of *S. spectabilis*, following the production at 7 different incubation days (7, 10, 14, 17, 21, 25 and 28), and testing two larger scale formats (250 and 500 mL Erlenmeyer flasks containing 50 and 100 mL of solid medium respectively) (Figure S.7). As for the OSMAC-based experiment, the production of $C_{28}H_{48}N_4O_7$ was measured with UHPLC-UV by comparing the areas under the peak to their corresponding control areas at 210 nm. Again, the relative production of the component was considerably higher for strain CF-278320 than for CBS 340.70T. The highest production titers for strain CF-278320 are reached between 14 and 21 days of fermentation with the 500 mL flask format, being the maximum value of 5 mg/L obtained at 17 days (Figure S.8).

Spectabilide A purification and structure elucidation

Crude extracts from the time course experiment in solid-state fermentation BRFT were processed to isolate the novel compound, designated as spectabilide A. The presence of this novel compound in one of the fractions derived from a reversed phase flash chromatography using C-18 Silica gel (Figure S.9) was confirmed by HPLC-HRMS and the fraction subsequently purified by repeated reversed phase semipreparative HPLC to yield spectabilide A as an amorphous pale-white solid.

Its (+)-ESI-TOF spectrum displayed a protonated adduct $[M + H]^+$ at m/z 553.3523 compatible with a molecular formula of $C_{28}H_{48}N_4O_7$ (Figure S.6). Analysis of its 1D and 2D NMR spectra (Figure S.11-17) identified signals compatible with the presence in the molecule of the aminoacids L-homoglutamine (HomoGln), and b-alanine (b-Ala) (Table 2, Figure 6). Signals of an olefinic methylene (d_H 5.75 and 5.29) that correlated in the HMBC spectrum to carbons at d_C 139.0 and 166.1 confirmed dehydroalanine (DHA) as an additional structural element of spectabilide A (Figure S.13). Finally, a unit of 3,5-dihydroxy-2,4-dimethyltetradecanoic acid (DHDMTDA) was also identified as part of the molecule based on correlations observed in the COSY and HMBC spectra (Figure 6b). HMBC correlations between H-1 of HomoGln and the carbonyl group of b-Ala, and between H-2 of b-Ala and the carbonyl of DHA established the sequence Homo Gln- b-Ala-DHA (Figure 6b). An additional HMBC correlation between H5 of the DHDMTDA moiety and the carbonyl of HomoGln established a lactone bridge between these two structural units. The low field chemical shift of H-5 (d_H 5.14) is also in agreement with this proposal. Finally, although no long-range correlations were observed in the HMBC spectrum to corroborate it, a second ring closure between the NH of DHA and the carbonyl group of DHDMTDA was proposed to comply with the molecular formula determined by HRMS. For the same reason, HomoGln instead of Homoglutamic acid was proposed as a structural element of spectabilide A. An L configuration was determined for L-HomoGln through Marfey's analysis (Figure S.18). Regarding the stereochemistry of DHDMTDA, a relative configuration 2*R*, 3*S*, 5*S* was tentatively proposed based on coupling constant analysis and NOESY correlations (Figure 6c). Thus, Large coupling constants of 10.8 and 10.7 Hz for the pairs H-5/H4a and H-3/H-4b, respectively, indicated an antiperiplanar disposition of these two pairs of hydrogens. NOESY correlations between H-2, H-3 and H-4a located these three hydrogens on the same face of the molecule (Figure S.14). Additional NOESY correlations between H-4b and H.5 and Me-15 located these groups on the other side of the molecule, completing the stereochemical

assignment of this part of the molecule. The stereochemistry at C-6 remained undetermined. Thus, the structure shown in figure 6a was proposed for spectabilide A.

Table 2. NMR spectroscopic data (CD₃OD, 500 MHz for ¹H, 125 MHz for ¹³C) of Figure 6

	Position	δ ¹ H, m, <i>J</i> (Hz)	δ ¹³ C, Mult	HMBC (H to C)
L - homoglutamine	1	4.24, dd (8.5, 5.4)	55.3, CH	C2, C3, CO, CO b-Ala
	2a	1.86, m	31.9, CH ₂	C1
	2b	1.75, m		C1, C3
	3a	1.75, m	23.4, CH ₂	C2, C4
	3b	1.67, m		C2, C4, C5
	4	2.25, brd t (7.0)	35.71, CH ₂	C2, C3, C5
	5		178.3, C	
	CO		173.4, C	
β -alanine	1a	2.51, ddd (16.6, 4.8, 2.3)	34.9, CH ₂	C2, CO
	1b	2.43, ddd (16.6, 10.8, 3.0)		
	2a	3.79, m	36.0, CH ₂	C1, CO, CO DHA
	2b	3.27, ddd (13.4, 10.8, 2.3)		C1, CO, CO DHA
	CO		175.2, C	
dehydroalanine	1		139.0, C	
	2a	5.75, s	115.0, CH ₂	CO
	2b	5.28, s		C1, CO
	CO		166.1, C	
DHDMTDA	1		177.0, C	
	2	2.66, qd (7.0, 4.6)	47.7, CH	C1, C3, C4, C15
	3	3.77, m	69.0, CH	C-1, C4, C5
	4a	1.99, ddd (14.2, 10.8, 1.7)	33.2, CH ₂	C5
	4b	1.52, ddd (14.2, 10.7, 1.9)		C3
	5	5.14, ddd (10.8, 4.9, 1.8)	76.8, CH	CO Homo-Gln, C3, C4, C6, C7, C16
	6	1.75, m	38.2, CH	
	7a	1.40, m	33.6, CH ₂	
	7b	1.14, m		C5
	8a	1.40, m	28.3, CH ₂	
	8b	1.28, m		
	9	1.24-1.34*	30.9, CH ₂	
	10	1.24-1.34*	31.1, CH ₂	
	11	1.24-1.34*	30.6, CH ₂	
12	1.24-1.34*	33.2, CH ₂		
13	1.24-1.34*	23.9, CH ₂		
14	0.90, t (6.6)	14.6, CH ₃	C12, C13	

	15	1.10, d (7.0)	11.4, CH ₃	C1, C2, C3
	16	0.89, d (6.8)	15.5, CH ₃	C5, C6, C7

*Overlapping signals.

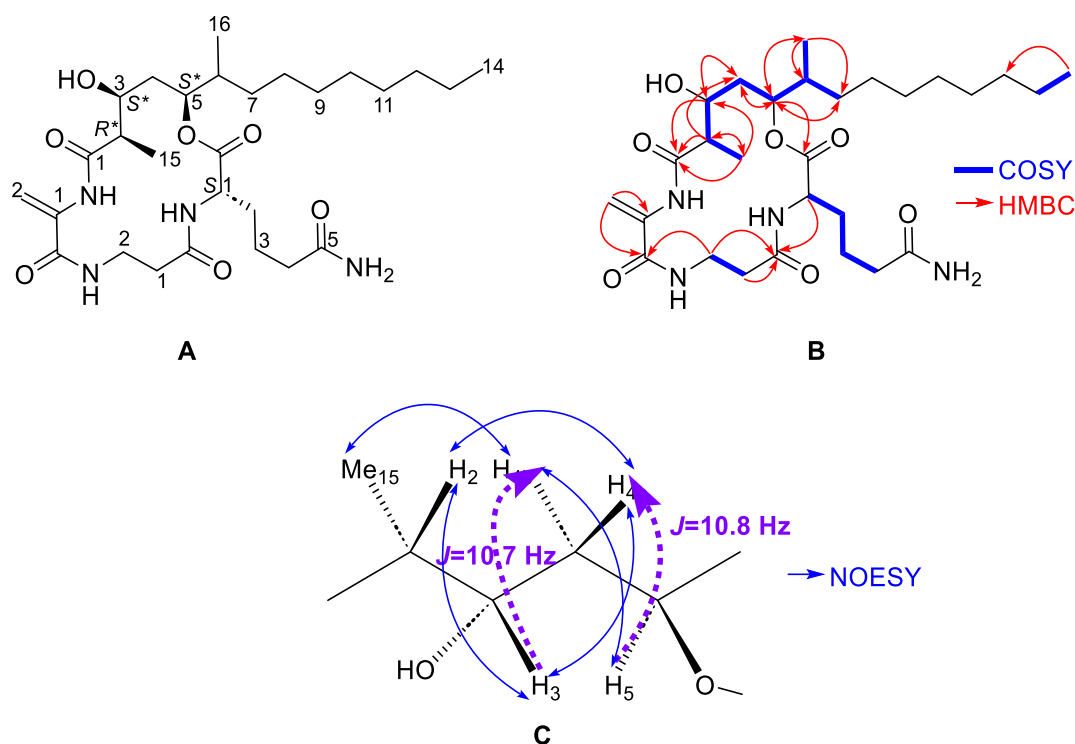


Figure 6. *A* Structure of spectabilide A; *B* Key COSY (bold blue) and HMBC (H to C, red) correlations observed in the structure of spectabilide A. *C* coupling constants and NOESY correlations observed around the C2-C6 fragment of DHDMTDA in spectabilide A.

Cytotoxicity bioassay

The activity of spectabilide A was evaluated against a panel of five different human cancer cell lines by means of the MTT reduction assay in a dose response curve. (Figure S.10). Spectabilide A showed potent activity against all cell lines tested, with reported ED₅₀ values of 0.28 μM (95% Confidence Interval (CI) 0.26-0.30 μM) for HepG2 (hepatocellular carcinoma), 0.11 μM (95% CI 0.11-0.11 μM) for MCF-7 (breast adenocarcinoma), 0.23 μM (95% CI 0.23-0.24 μM) for MIA PaCa-2 (pancreas carcinoma), 0.13 μM (95% CI 0.13-0.13 μM) for A2058 (skin melanoma), and 0.16 μM (95% CI 0.15-0.16 μM) for A549 (lung carcinoma).

Discussion

The OSMAC approach applied to *S. spectabile* strains CF-278320 and CBS 340.70T resulted in the expansion of the chemical diversity produced by the fungus, as shown on Figure 4 by the different SMs produced in the different fermentation conditions. The use of FFBiolog microplates allowed us to explore the preferences of the strains in terms of carbon and nitrogen sources, generating the necessary information to tailor the panel of

fermentation media designed for the OSMAC-based media study. Once again, the OSMAC approach proved to be an excellent tool to increase the diversity on the metabolic profiles generated by the studied strain, highlighting the impact that fermentation parameters have on the expression of biosynthetic genes. For instance, MV8 and WS80 media triggered the production of annotated components such as trichodermol, trichoverrol A, verrucarín A and myrotoxin, while other starch rich media like BRFT and Wheat-1 stimulated the mycelia growth while inhibiting the production of most toxins (Table S.1). It is known that media formulations containing a considerable amount of carbon and nitrogen sources support fungal growth at the expense of sporulation and, as a result, reduce the production of mycotoxins, or secondary metabolites in general (Tribelhorn, 2023; Calvo, 2002; Brodhagen, 2006). In this study we also observed that the addition of SAHA can inhibit the production of secondary metabolites, as seen for several components and toxins on the CYS80 and SXSX media, or enhance it, as shown by the production of verrucarín J and trichodepsipeptide B on the FOF medium. It has been reported that the perturbation of the normal state of chromatin in filamentous fungi can interfere with its regulatory functions, thus sometimes leading to the activation of cryptic regions of the chromosome (Brosch et al., 2008). Epigenetic modifiers like the DNMT inhibitor hydralazine hydrochloride or the HDAC inhibitor SAHA have been successfully used to modulate the chromatin dynamics and stimulate the expression of silent genes (Scherlach and Hertweck, 2009; Cichewicz, 2010; González-Menéndez et al., 2016). On the other hand, the addition of small amounts of adsorptive polymeric resins, such as XAD-16 or HP-20, to the fermentation media can improve the production of certain metabolites by sequestering them, preventing both their degradation and toxic effects for the cell (Marshall et al. 1990; Phillips et al. 2013; González-Menéndez et al. 2014), even though in this study we were not able to observe any significant change due to the addition of XAD-16.

Efficient and consistent dereplication methods combined with powerful tools and broad databases such as GNPS, the DNP, and NPAtlas, facilitate the identification of known and unknown molecules, and the understanding of how they cluster to each other. This allowed to reveal the presence of putative mycotoxins and other SMs produced by the strains. Among these molecules we identified the trichothecenes roridin, 8- α -acetoxyverrol, trichoverrol, trichodermol, and verrucarín, a group of fungal toxins produced by species of the genera *Fusarium*, *Myrothecium*, *Spicellum*, *Stachybotrys*, *Cephalosporium*, *Trichoderma*, and *Trichothecium* (McCormick et al., 2011; Richardson et al., 1989). SMs such as trichodepsipeptide B and guangomide B are instead characteristic of the *Trichothecium* genus (Sy-Cordero et al., 2011; Springer et al., 1984). The presence of these chemotaxonomic biomarker toxins is in contrast with the original classification of *S. spectabile* (CBS 340.70T) as a member of the *Stanjemonium* clade and strengthen the reclassification that was already proposed by Hou et al. in 2023. The relocation of *S. spectabile* from the *Stanjemonium* clade towards the *Trichothecium* clade is additionally supported by its position in the phylogenetic tree (Figure 2). Other compounds, such as trichodermol, 8- α -acetoxyverrol, verrol, and verrucarín L-acetate, were previously found by Krohn et al. (2003) in the fermentation extracts of *A. spectabile* NBRC101148, and this only confirms the synonymy of *A. spectabile* with *S. spectabile*. As an additional support for the reclassification proposal, other members of the *Stanjemonium* genus, like *S. grisellum*, are known to produce peptaibols (Sánchez-Giraldo, L.M., 2023), a group of polypeptides with antimicrobial activity, typically produced by *Trichoderma* and *Emericellopsis* genera (Molnár et al., 2010;

<https://peptaibol.cryst.bbk.ac.uk/introduction.htm>), which are completely absent in the examined strains of *S. spectabile* CF-278320 and CBS 340.70T.

OSMAC and metabolomic approaches allowed us to discover a novel cytotoxic compound, spectabilide A, and its cluster of analogues. Spectabilide A belongs to the group of cyclic lipodepsipeptides, a large family of peptide-derived compounds that show a wide range of biological activities, such as antimicrobial, immunosuppressive, cytotoxic, and antitumoral. They are broadly distributed and mainly produced by bacteria, marine organisms and filamentous fungi. These compounds are usually biosynthesized by the combination of a non-ribosomal peptide synthetase (NRPS) synthesizing the aminoacidic moiety and a polyketide synthase (PKS) involved in the fatty acid synthesis (Sivatharushan, S. and Scherkenbeck, J., 2014; Wang, X. et al., 2018; Kitagaki, J. et al., 2015; Bionda, N. et al., 2013; Evidente, A., 2022). The compound has a simple structure, composed of a hydroxylated fatty acid chain linked to a chain of three amino acids: dehydroalanine, β -alanine, and homoglutamine. This structure resembles that of fusaristatins, a group of metabolites produced by *Fusarium* spp., which also belongs to the *Hypocreales* order (Shiono, Y. et al., 2007). Referring to the reported bioactivity of fusaristatins, we tested the cytotoxic activity of spectabilide A against a panel of five human tumour cell lines. The novel compound displayed potent cytotoxicity, with the strongest activity ($ED_{50} = 0.11 \mu\text{M}$) against the MCF-7 breast adenocarcinoma cell line. For instance, the anti-tumour effects reported in literature for fusaristatins A and B against LU 65 lung cancers cells were much weaker, with IC_{50} values of $23 \mu\text{M}$ and $7 \mu\text{M}$, respectively (Shiono, Y. et al., 2007).

Conclusions

In this study, we have demonstrated that the combination of OSMAC and metabolomic approaches is still a valuable method to expand the chemical diversity produced by a poorly studied fungus, *S. spectabile*, allowing to enrich its chemical space with several molecules that are poorly produced or not produced at all under standard cultivation conditions.

The extensive analysis we carried out on the fermentation extracts of the strains also revealed the presence of a novel cyclic depsipeptide, spectabilide A, exhibiting a potent cytotoxic activity against a panel of tumoral cell lines, suggesting a potential pharmacological interest for the molecule. Moreover, the information we gathered from the phylogenetic and chemotaxonomic analyses further support the reclassification of *S. spectabile* as a new member of the genus *Trichothecium*, in accordance with previous studies.

The production of spectabilide A by *S. spectabile* highlights the ability of plant associated fungi to produce novel molecules of interest with different biological activities, and of high relevance for the field of drug discovery. Further studies are needed to define the biosynthetic process behind the production of the novel cyclodepsipeptide, as well as to explore the unexpressed biosynthetic potential of *S. spectabile* strains. Nevertheless, this

study highlighted the value of using different culture-based strategies to stimulate the metabolic potential of species from poorly studied ecological niches and discover new secondary metabolites.

Acknowledgements

The authors have no support to report.

References

Al Samra L, El Nahas M, Mneimneh I, Sinno A, Tokajian S, Rahy K, Thoumi S, Ali L, Yammine W, Al Khoury C (2025) Evaluation of Beauvericin's activity and mode of action against all life stages of *L. tropica* for cutaneous Leishmaniasis therapy. *Frontiers in Cellular and Infection Microbiology* 15. <https://doi.org/10.3389/fcimb.2025.1599766>

Bacon CW (1988) Procedure for isolating the endophyte from tall fescue and screening isolates for ergot alkaloids. *Applied and Environmental Microbiology* 54: 2615–2618. <https://doi.org/10.1128/aem.54.11.2615-2618.1988>

Bills GF, González Menéndez V, Platas G (2012) *Kabatiella bupleuri* sp. nov. (Dothideales), a pleomorphic epiphyte and endophyte of the Mediterranean plant *Bupleurum gibraltarium* (Apiaceae). *Mycologia* 104: 962–973. <https://doi.org/10.3852/12-003>

Bills GF, Platas G, Fillola A, Jiménez MR, Collado J, Vicente F, Martín J, González A, Bur-Zimmermann J, Tormo JR, Peláez F (2008) Enhancement of antibiotic and secondary metabolite detection from filamentous fungi by growth on nutritional arrays. *Journal of Applied Microbiology* 104: 1644–1658. <https://doi.org/10.1111/j.1365-2672.2008.03735.x>

Bionda N, Pitteloud J-P, Cudic P (2013) Cyclic lipodepsipeptides: a new class of antibacterial agents in the battle against resistant bacteria. *Future medicinal chemistry* 5: 10.4155/fmc.13.86. <https://doi.org/10.4155/fmc.13.86>

Bode HB, Bethe B, Höfs R, Zeeck A (2002) Big Effects from Small Changes: Possible Ways to Explore Nature's Chemical Diversity. *ChemBioChem* 3: 619. [https://doi.org/10.1002/1439-7633\(20020703\)3:7%3C619::aid-cbic619%3E3.0.co;2-9](https://doi.org/10.1002/1439-7633(20020703)3:7%3C619::aid-cbic619%3E3.0.co;2-9)

Böhler P, Stuhldreier F, Anand R, Kondadi AK, Schlütermann D, Berleth N, Deitersen J, Wallot-Hieke N, Wu W, Frank M, Niemann H, Wesbuer E, Barbian A, Luyten T, Parys JB, Weidtkamp-Peters S, Borchardt A, Reichert AS, Peña-Blanco A, García-Sáez AJ

(2018) The mycotoxin phomoxanthone A disturbs the form and function of the inner mitochondrial membrane. *Cell Death & Disease* 9. <https://doi.org/10.1038/s41419-018-0312-8>

Brodhagen M, Keller NP (2006) Signalling pathways connecting mycotoxin production and sporulation. *Molecular Plant Pathology* 7: 285–301. <https://doi.org/10.1111/j.1364-3703.2006.00338.x>

Brosch G, Loidl P, Graessle S (2008) Histone modifications and chromatin dynamics: a focus on filamentous fungi. *FEMS Microbiology Reviews* 32: 409–439. <https://doi.org/10.1111/j.1574-6976.2007.00100.x>

Calvo AM, Wilson RA, Bok JW, Keller NP (2002) Relationship between Secondary Metabolism and Fungal Development. *Microbiology and Molecular Biology Reviews* 66: 447–459. <https://doi.org/10.1128/mmbr.66.3.447-459.2002>

Cautain B, de Pedro N, Schulz C, Pascual J, da S. Sousa T, Martin J, Pérez-Victoria I, Asensio F, González I, Bills GF, Reyes F, Genilloud O, Vicente F (2015) Identification of the Lipodepsipeptide MDN-0066, a Novel Inhibitor of VHL/HIF Pathway Produced by a New *Pseudomonas* Species. Dahiya R (Ed.). *PLOS ONE* 10: e0125221. <https://doi.org/10.1371/journal.pone.0125221>

Chambers MC, Maclean B, Burke R, Amodei D, Ruderman DL, Neumann S, Gatto L, Fischer B, Pratt B, Egertson J, Hoff K, Kessner D, Tasman N, Shulman N, Frewen B, Baker TA, Brusniak M-Y, Paulse C, Creasy D, Flashner L (2012) A cross-platform toolkit for mass spectrometry and proteomics. *Nature Biotechnology* 30: 918–920. <https://doi.org/10.1038/nbt.2377>

Chandra S (2012) Endophytic fungi: novel sources of anticancer lead molecules. *Applied Microbiology and Biotechnology* 95: 47–59. <https://doi.org/10.1007/s00253-012-4128-7>

Cichewicz RH (2010) Epigenome manipulation as a pathway to new natural product scaffolds and their congeners. *Nat. Prod. Rep.* 27: 11–22. <https://doi.org/10.1039/b920860g>

de Pedro N, Cautain B, Melguizo A, Cortes D, Vicente F, Genilloud O, Tormo JR, Peláez F (2012) Analysis of cytotoxic activity at short incubation times reveals profound differences among *Annonaceus* acetogenins, inhibitors of mitochondrial Complex I. *Journal of Bioenergetics and Biomembranes* 45: 145–152. <https://doi.org/10.1007/s10863-012-9490-8>

Evidente A (2022) Bioactive Lipodepsipeptides Produced by Bacteria and Fungi. *International Journal of Molecular Sciences* 23: 12342–12342. <https://doi.org/10.3390/ijms232012342>

Farinella VF, Kawafune ES, Tangerina MMP, Domingos HV, Costa-Lotufu LV, Ferreira MJP (2021) OSMAC Strategy Integrated with Molecular Networking for Accessing Griseofulvin Derivatives from Endophytic Fungi of *Moquiniastrum polymorphum* (Asteraceae). *Molecules* 26: 7316. <https://doi.org/10.3390/molecules26237316>

Fredimoses M, Zhou X, Ai W, Tian X, Yang B, Lin X, Liu J, Liu Y (2018) Emerixanthone E, a new xanthone derivative from deep sea fungus *Emericella* sp SCSIO 05240. *Natural product research* 33: 2088–2094. <https://doi.org/10.1080/14786419.2018.1487966>

Gams W (1973) Phialides with Solitary conidia? Remarks on Conidium Ontogeny in Some Hyphomycetes. 7: 161–169.

Gams W, O'Donnell K, Schroers H-J, Christensen M (1998) Generic classification of some more hyphomycetes with solitary conidia borne on phialides. *Canadian Journal of Botany* 76: 1570–1583. <https://doi.org/10.1139/b98-104>

Georgousaki K, Tsafantakis N, Gumeni S, Lambrinidis G, González-Menéndez V, Tormo JR, Genilloud O, Trougakos IP, Fokialakis N (2020) Biological Evaluation and In Silico Study of Benzoic Acid Derivatives from *Bjerkandera adusta* Targeting Proteostasis Network Modules. *Molecules* 25: 666. <https://doi.org/10.3390/molecules25030666>

Georgousaki K, Tsafantakis N, Gumeni S, González-Menéndez V, Pedro N de, Tormo JR, Almeida C, Lambert C, Genilloud O, Trougakos IP, Fokialakis N (2019) *Cercospora* sp. as a source of anti-aging polyketides targeting 26S proteasome and scale-up production in submerged bioreactor. *Journal of Biotechnology* 301: 88–96. <https://doi.org/10.1016/j.jbiotec.2019.05.015>

Gonzalez-Menendez V, Martin J, Siles JA, Gonzalez-Tejero MR, Reyes F, Platas G, Tormo JR, Genilloud O (2017) Biodiversity and chemotaxonomy of *Preussia* isolates from the Iberian Peninsula. *Mycological Progress* 16: 713–728. <https://doi.org/10.1007/s11557-017-1305-1>

González-Menéndez V, Pérez-Bonilla M, Pérez-Victoria I, Martín J, Muñoz F, Reyes F, Tormo J, Genilloud O (2016) Multicomponent Analysis of the Differential Induction of Secondary Metabolite Profiles in Fungal Endophytes. *Molecules* 21: 234. <https://doi.org/10.3390/molecules21020234>

González-Menéndez V, Asensio F, Moreno C, Pedro N de, Monteiro MC, de la Cruz M, Vicente F, Bills GF, Reyes F, Genilloud O, Tormo JR (2014) Assessing the effects of adsorptive polymeric resin additions on fungal secondary metabolite chemical diversity. *Mycology: An International Journal on Fungal Biology* 5: 179–191. <https://doi.org/10.1080/21501203.2014.942406>

González-Menéndez V, Crespo G, de Pedro N, Diaz C, Martín J, Serrano R, Mackenzie TA, Justicia C, González-Tejero MR, Casares M, Vicente F, Reyes F, Tormo JR, Genilloud O (2018) Fungal endophytes from arid areas of Andalusia: high potential sources for antifungal and antitumoral agents. *Scientific Reports* 8. <https://doi.org/10.1038/s41598-018-28192-5>

Hashem AH, Attia M, Kandil EK, Fawzi MM, Abdelrahman AS, Khader MS, Khodaira MA, Emam AE, Goma MA, Abdelaziz AM (2023) Bioactive compounds and biomedical applications of endophytic fungi: a recent review. *Microbial Cell Factories* 22. <https://doi.org/10.1186/s12934-023-02118-x>

Hewage RT, Aree T, Mahidol C, Ruchirawat S, Kittakoop P (2014) One strain-many compounds (OSMAC) method for production of polyketides, azaphilones, and an isochromanone using the endophytic fungus *Dothideomycete* sp. *Phytochemistry* 108: 87–94. <https://doi.org/10.1016/j.phytochem.2014.09.013>

Hou LW, Giraldo A, Groenewald JZ, Rämä T, Summerbell RC, Huang GZ, Cai L, Crous PW (2023) Redisposition of acremonium-like fungi in *Hypocreales*. *Studies in Mycology* 105: 23–203. <https://doi.org/10.3114/sim.2023.105.02>

Kildgaard S, Mansson M, Dosen I, Klitgaard A, Frisvad J, Larsen T, Nielsen K (2014) Accurate Dereplication of Bioactive Secondary Metabolites from Marine-Derived Fungi by UHPLC-DAD-QTOFMS and a MS/HRMS Library. *Marine Drugs* 12: 3681–3705. <https://doi.org/10.3390/md12063681>

Kitagaki J, Shi G, Miyauchi S, Murakami S, Yang Y (2015) Cyclic depsipeptides as potential cancer therapeutics. *Anti-Cancer Drugs* 26: 259–271. <https://doi.org/10.1097/cad.0000000000000183>

Krohn K, Steingröver K, Aust H-J, Draeger S, Schulz B (2003) Biologically Active Metabolites from Fungi, 17. 8- α -Acetoxyverrol, A new Member of the Trichothecene Sesquiterpenes. *Natural Product Research* 17: 67–70. <https://doi.org/10.1080/1478641031000062223>

Kubicek CP, Bissett J, Druzhinina I, Kullnig-Gradinger C, Szakacs G (2003) Genetic and metabolic diversity of *Trichoderma*: a case study on South-East Asian isolates. *Fungal Genetics and Biology* 38: 310–319. [https://doi.org/10.1016/s1087-1845\(02\)00583-2](https://doi.org/10.1016/s1087-1845(02)00583-2)

Li JY, Strobel GA (2001) Jesterone and hydroxy-jesterone antioomycete cyclohexenone epoxides from the endophytic fungus *Pestalotiopsis jesteri*. *Phytochemistry* 57: 261–265. [https://doi.org/10.1016/s0031-9422\(01\)00021-8](https://doi.org/10.1016/s0031-9422(01)00021-8)

Marshall VP, McWethy SJ, Sirotti JM, Cialdella JI (1990) The effect of neutral resins on the fermentation production of rubradirin. *Journal of Industrial Microbiology & Biotechnology* 5: 283–287. <https://doi.org/10.1007/bf01578202>

Martín J, Crespo G, González-Menéndez V, Pérez-Moreno G, Sánchez-Carrasco P, Llamas I, Ruiz-Pérez LM, González-Pacanowska D, Vicente F, Genilloud O, Bills GF, Reyes F (2014) MDN-0104, an Antiplasmodial Betaine Lipid from *Heterospora chenopodii*. 77: 2118–2123. <https://doi.org/10.1021/np500577v>

Masouka Y, Shin-Ya K, Fimihata K, Matsumo H, Takebayashi Y, Nagai K, Suzuki K-I, Hayakawa Y, Seto H (2000) Diheteropeptin, a Novel Substance with TGF- β -like Activity, Produced by a Fungus, *Diheterospora chlamydosporia*. II. Physico-chemical Properties and Structure Elucidation. *The Journal of Antibiotics* 53: 793–798. <https://doi.org/10.7164/antibiotics.53.793>

McCormick SP, Stanley AM, Stover NA, Alexander NJ (2011) Trichothecenes: From Simple to Complex Mycotoxins. *Toxins* 3: 802–814. <https://doi.org/10.3390/toxins3070802>

Meng T-X, Ishikawa H, Shimizu K, Ohga S, Kondo R (2011) A glucosylceramide with antimicrobial activity from the edible mushroom *Pleurotus citrinopileatus*. *Journal of Wood Science* 58: 81–86. <https://doi.org/10.1007/s10086-011-1213-y>

Molnár I, Gibson DM, Krasnoff SB (2010) Secondary metabolites from entomopathogenic Hypocrealean fungi. *Natural Product Reports* 27: 1241. <https://doi.org/10.1039/c001459c>

Mosmann T (1983) Rapid colorimetric assay for cellular growth and survival: Application to proliferation and cytotoxicity assays. *Journal of Immunological Methods* 65: 55–63. [https://doi.org/10.1016/0022-1759\(83\)90303-4](https://doi.org/10.1016/0022-1759(83)90303-4)

Nguyen L-T, Schmidt HA, von Haeseler A, Minh BQ (2014) IQ-TREE: A Fast and Effective Stochastic Algorithm for Estimating Maximum-Likelihood Phylogenies. *Molecular Biology and Evolution* 32: 268–274. <https://doi.org/10.1093/molbev/msu300>

Nylander JAA (2004) MrModeltest v2.

Ondeyka JG, Zink D, Basilio A, Vicente F, Bills G, Diez MT, Motyl M, Gabe Dezeny, Byrne K, Singh SB (2007) Coniothyron, a Chlorocyclopentandienylbenzopyrone as a Bacterial Protein Synthesis Inhibitor Discovered by Antisense Technology. *Journal of Natural Products* 70: 668–670. <https://doi.org/10.1021/np060557d>

Papaspyridi L-M, Katapodis P, Gonou-Zagou Z, Kapsanaki-Gotsi E, Christakopoulos P (2010) Optimization of biomass production with enhanced glucan and dietary fibres content by *Pleurotus ostreatus* ATHUM 4438 under submerged culture. *Biochemical Engineering Journal* 50: 131–138. <https://doi.org/10.1016/j.bej.2010.04.008>

Paranagama PA, Wijeratne EMK, Gunatilaka AAL (2007) Uncovering Biosynthetic Potential of Plant-Associated Fungi: Effect of Culture Conditions on Metabolite Production by *Paraphaeosphaeria quadrisepata* and *Chaetomium chiversii*. *Journal of Natural Products* 70: 1939–1945. <https://doi.org/10.1021/np070504b>

Paredes G (2024) SNA (Synthetic Nutrient Deficient) Agar for Identification fungi v1. <https://doi.org/10.17504/protocols.io.261ge5jkjg47/v1>

Peláez F, Cabello A, Platas G, Díez MT, González del Val A, Basilio A, Martín I, Vicente F, Bills GE, Giacobbe RA, Schwartz RE, Onish JC, Mainz MS, Abruzzo GK, Flattery AM, Kong L, Kurtz MB (2000) The discovery of enfumafungin, a novel antifungal compound produced by an endophytic *Hormonema* species biological activity and taxonomy of the producing organisms. *Systematic and Applied Microbiology* 23: 333–343. [https://doi.org/10.1016/s0723-2020\(00\)80062-4](https://doi.org/10.1016/s0723-2020(00)80062-4)

Pérez-Victoria I, Martín J, Reyes F (2016) Combined LC/UV/MS and NMR Strategies for the Dereplication of Marine Natural Products. *Planta Medica* 82: 857–871. <https://doi.org/10.1055/s-0042-101763>

Phillips T, Chase M, Wagner S, Renzi C, Powell M, DeAngelo J, Michels P (2013) Use of in situ solid-phase adsorption in microbial natural product fermentation development. *Journal of Industrial Microbiology and Biotechnology* 40: 411–425. <https://doi.org/10.1007/s10295-013-1247-9>

Poynton EF, van Santen JA, Pin M, Contreras MM, McMann E, Parra J, Showalter B, Zaroubi L, Duncan K, Linington RG (2024) The Natural Products Atlas 3.0: extending the database of microbially derived natural products. *Nucleic Acids Research* 53: D691–D699. <https://doi.org/10.1093/nar/gkae1093>

Richardson B, Hsieh G-C, Jarvis BB, Sharma RP (1989) Effects of macrocyclic trichothecene mycotoxins on the murine immune system. *Archives of Environmental Contamination and Toxicology* 18: 388–395. <https://doi.org/10.1007/bf01062363>

Sánchez Giraldo LM (2024) New Peptpabiotics from Stanjemonium Strains Isolated from Lichens, as New Agents against Tomato Phytpathogen *Clavibacter Michiganensis* Subsp. *Michiganensis*.

Scherlach K, Hertweck C (2009) Triggering cryptic natural product biosynthesis in microorganisms. *Organic & Biomolecular Chemistry* 7: 1753. <https://doi.org/10.1039/b821578b>

Shannon P, Markiel A, Ozier O, Baliga NS, Wang JT, Ramage D, Amin N, Schwikowski B, Ideker T (2003) Cytoscape: a Software Environment for Integrated Models of Biomolecular Interaction Networks. *Genome Research* 13: 2498–2504. <https://doi.org/10.1101/gr.1239303>

Shiono Y, Tsuchinari M, Shimanuki K, Miyajima T, Murayama T, Koseki T, Laatsch H, Funakoshi T, Takanami K, Suzuki K (2007) Fusaristatins A and B, Two New Cyclic Lipopeptides from an Endophytic *Fusarium* sp. *ChemInform* 38. <https://doi.org/10.1002/chin.200746163>

Singh SB, Ondeyka JG, Harris GH, Herath K, Zink DL, Vicente F, Bills GF, Collado J, Platas G, González A, Jesús Martín, Reyes F, Wang H, Jennifer Nielsen Kahn, Galuska S, Giacobbe RA, Abruzzo GK, Roemer T, Xu D (2012) Isolation, Structure, and Biological Activity of Phaeofungin, a Cyclic Lipodepsipeptide from a *Phaeosphaeria* sp. Using the Genome-Wide *Candida albicans* Fitness Test. *Journal of Natural Products* 76: 334–345. <https://doi.org/10.1021/np300704s>

Sivanathan S, Scherkenbeck J (2014) Cyclodepsipeptides: A Rich Source of Biologically Active Compounds for Drug Research. *Molecules* 19: 12368–12420. <https://doi.org/10.3390/molecules190812368>

Springer JP, Cole R, Dorner JW, Cox RH, Richard J, Barnes CL, van (1984) Structure and conformation of roseotoxin B. *Journal of the American Chemical Society* 106: 2388–2392. <https://doi.org/10.1021/ja00320a028>

Suay I, Arenal F, Asensio FJ, Basilio A, Angeles Cabello M, Teresa Díez M, García JB, González del Val A, Gorrochategui J, Hernández P, Peláez F, Francisca Vicente M (2000) Screening of basidiomycetes for antimicrobial activities. *Antonie van Leeuwenhoek* 78: 129–140. <https://doi.org/10.1023/A:1026552024021>

Sy-Cordero AA, Graf TN, Adcock AF, Kroll DJ, Shen Q, Swanson SM, Wani MC, Pearce CJ, Oberlies NH (2011) Cyclodepsipeptides, Sesquiterpenoids, and Other Cytotoxic Metabolites from the Filamentous Fungus *Trichothecium* sp. (MSX 51320). *Journal of Natural Products* 74: 2137–2142. <https://doi.org/10.1021/np2004243>

Tribelhorn K, Twarużek M, Kosicki R, Straubinger RK, Ebel F, Ulrich S (2023) A Chemically Defined Medium That Supports Mycotoxin Production by *Stachybotrys chartarum* Enabled Analysis of the Impact of Nitrogen and Carbon Sources on the Biosynthesis of Macrocyclic Trichothecenes and Stachybotrylactam. *Applied and Environmental Microbiology* 89. <https://doi.org/10.1128/aem.00163-23>

Wang M, Carver JJ, Phelan VV, Sanchez LM, Garg N, Peng Y, Nguyen DD, Watrous J, Kapono CA, Luzzatto-Knaan T, Porto C, Bouslimani A, Melnik AV, Meehan MJ, Liu W-T, Crüsemann M, Boudreau PD, Esquenazi E, Sandoval-Calderón M, Kersten RD (2016) Sharing and community curation of mass spectrometry data with Global Natural Products Social Molecular Networking. *Nature Biotechnology* 34: 828–837. <https://doi.org/10.1038/nbt.3597>

Wang X, Gong X, Li P, Lai D, Zhou L (2018) Structural Diversity and Biological Activities of Cyclic Depsipeptides from Fungi. *Molecules* 23: 169. <https://doi.org/10.3390/molecules23010169>

Yuan S, Gopal JV, Ren S, Chen L, Liu L, Gao Z (2020) Anticancer fungal natural products: Mechanisms of action and biosynthesis. *European Journal of Medicinal Chemistry* 202: 112502–112502. <https://doi.org/10.1016/j.ejmech.2020.112502>

Supporting Information

Supporting information are reported on Supplementary Materials.